PROTEIN STRUCTURE REPORTS

Crystal structure of the fungal nitroreductase Frm2 from *Saccharomyces cerevisiae*

Hyung-Nam Song,[1,2] Dae-Gwin Jeong,[1,3] Seo-Young Bang,[1] Se-Hwan Paek,[2] Byoung-Chul Park,[1,3] Sung-Goo Park,[1,3]* and Eui-Jeon Woo[1,3]*

[1]Korea Research Institute of Bioscience and Biotechnology, Daejeon 305-806, Republic of Korea
[2]Department of Biotechnology and Bioinformatics, Korea University, Sejong 339-700, Republic of Korea
[3]Bio-Analytical Science Division, Korea University of Science and Technology (UST), Daejeon, Republic of Korea

Received 26 December 2014; Accepted 31 March 2015
DOI: 10.1002/pro.2686
Published online 11 April 2015 proteinscience.org

Abstract: Nitroreductases are flavoenzymes that catalyze nitrocompounds and are widely utilized in industrial applications due to their detoxification potential and activation of biomedicinal prodrugs. Type I nitroreductases are classified into subgroups depending on the use of NADPH or NADH as the electron donor. Here, we report the crystal structure of the fungal nitroreductase Frm2 from *Saccharomyces cerevisiae*, one of the uncharacterized subgroups of proteins, to reveal its minimal architecture previously observed in bacterial nitroreductases such as CinD and YdjA. The structure lacks protruding helical motifs that form part of the cofactor and substrate binding site, resulting in an open and wide active site geometry. Arg82 is uniquely conserved in proximity to the substrate binding site in Frm2 homologues and plays a crucial role in the activity of the active site. Frm2 primarily utilizes NADH to reduce 4-NQO. Because missing helical elements are involved in the direct binding to the NAD(P)H in group A or group B in Type I family, Frm2 and its homologues may represent a distinctive subgroup with an altered binding mode for the reducing compound. This result provides a structural basis for the rational design of novel prodrugs with the ability to reduce nitrogen-containing hazardous molecules.

Keywords: nitroreductase; crystal structure; 4-nitroquinoline 1-oxide; NADH; *Saccharomyces cerevisiae*

Introduction

Nitroreductases reduce the nitrogen substituted compounds such as furazones, nitroaromatic compounds, flavins and ferricyanide by utilizing FMN as a cofactor and NAD(P)H as the reducing agent.[1,2] Nitrogen substituted compounds are widely present in the environment and are involved in a range of industrial process such as explosives, pesticides, antimicrobial agents, pharmaceuticals, food additives, and dyes.[3–5] Nitroreductases in bacteria are

Additional Supporting Information may be found in the online version of this article.

Grant sponsor: The KRIBB Research Initiative Program.

*Correspondence to: Eui-Jeon Woo; Korea Research Institute of Bioscience and Biotechnology, Daejeon 305-806, Republic of Korea. E-mail: ejwoo@kribb.re.kr or Sung-Goo Park; Korea Research Institute of Bioscience and Biotechnology, Daejeon 305-806, Republic of Korea. E-mail: sgpark@kribb.re.kr

classified into two families in which Type I nitroreductases catalyze the reduction of organic nitro compounds using a two-electron transfer mechanism, whereas Type II catalyzes a one electron reduction of the nitro group to produce nitro anion radicals. Almost all Type I oxygen insensitive nitroreductases share similar biochemical properties, such as a homodimeric association, broad substrate specificity and the catalytic reaction using a ping-pong bi-bi kinetic mechanism.[6–8] Type I can be classified into two main groups, Groups A and B, according to their similarity with *E. coli* nitroreductases NfsA and NfsB, respectively.[7] Group A uses NADPH as a reducing agent, whereas Group B can use either NADH or NADPH. Groups A and B share very low sequence identity with one another, despite some biochemical similarities.[9] Recently, an additional uncharacterized putative nitroreductase-like protein family including fungal proteins of Frm2 and Hbn1 was identified using sensitive methods of phylogenetic analysis in bacterial and eukaryotic genome databases.[10,11] These proteins, termed nitroreductase-like A proteins (NrlA), have similar physical and chemical properties as determined from the hydrophobic cluster analysis pattern and are suggested to be involved in maintaining the oxidative and/or nitrosative balance within cells. No structure is available for eukaryotic nitroreductases, and few data exist on the distribution of nitroreductase-like proteins in eukaryotic cells. In the yeast *Saccharomyces cerevisiae*, two proteins, Frm2 and Hbn1, sharing sequence homology of 59% identity, were identified as influencing the response to oxidative stress by modulating the GSH contents and antioxidant enzymatic activities such as SOD, CAT, and GPx.[9] Frm2 has low sequence homology and does not belong to either of the subgroups in the Type I family. We have previously reported on the enzymatic function of Frm2 as a novel nitroreductase that catalyzes 4-nitroquinoline-*N*-oxide (4-NQO) using NADH. LC–MS analysis indicated that Frm2 reduced 4-NQO substrate into 4-aminoquinoline-*N*-oxide (4-AQO) via 4-hydroxyaminoquinoline (4-HAQO).[12] A Frm2 deletion mutant exhibited growth inhibition in the presence of 4-NQO, demonstrating its involvement in the oxidative stress defense system. In the present study, we have determined the structure of Frm2 and compared it to other nitroreductases in Groups A and B of the Type I family to understand the functional and biochemical relevance of the protein and, thus, its activity.

Results

Overall structure of wild-Frm2

The crystal structure of Frm2 was determined in the absence of the FMN cofactor at a 3.0 Å resolution by molecular replacement. Frm2 forms a homodimer and the monomer possesses a typical nitroreductase motif ($\alpha + \beta$ fold) with the active site sandwiched at the dimer interface. Antiparallel beta strands of the core motif are surrounded by two long and five short helices. The beta strand at the C-terminus extends across the N-domain of the neighboring monomer to form a beta sheet core. A disordered loop in the region of 174–185 was not traced and is thus missing in the final model. The structure shows an obvious binding groove for the FMN cofactor that is surrounded by a loop of the α2 helix—β1 strand, α6 helix of one monomer, and β3 strand from a neighboring subunit [Fig. 1(A)]. A positively charged surface originating from Arg14 and Arg15 is located deep inside the cavity in a position to coordinate the phosphate group of the FMN cofactor. Based on the superposition to the FMN 4–NQO complex structure of CinD, Leu145, and Gln146 are located in the surface of the si face for the FMN isoalloxazine ring with Thr16, Arg82, His147 in the same face, while the Phe48 and Cys120 positions in the re face of the isoalloxazine ring.[13] The homodimeric interface forms the active site pocket in which Trp133, His147, Leu145, Gln146, and Pro45 from one subunit constitutes the FMN binding site with the other subunit. The conserved Arg 14 originating from an adjacent subunit is well positioned for direct binding to the FMN phosphate group. In comparison to other available structures in Group A (PDB code 3n2s, 1f5v, 3qdl) and Group B (1icu, 1vfr, 1kqd, 2wzw), Frm2 and its homologues exhibit conserved residues such as Tyr 18, which is involved in the interaction to O_2 of the isoalloxazine ring based on the CinD structure superposition, and Phe48, which is involved in the stacking interaction to the 4-NQO substrate [Fig. 1(B)]. In addition, it has a His147 located at the si face of the ring that is replaced by Glu in Group B and to Gly in Group A. Both Frm2 and CinD catalyze the 4-NQO substrate. The position of Arg82, which corresponds to the Lys 88 residue [Supporting Information Fig. S1], is in proximal position to the 4-NQO in CinD, which suggests its involvement in the reduction of the NO_2 moiety to NH2 for the conversion of 4-NQO to 4-AQO. Interestingly, this positively conserved charged residue is substituted to Asn in Group B and to residue Gln or Asn in Group A. To investigate the functional role of this residue, we generated the mutant of R82A and R82E and assayed the nitroreductase activity. When compared to wild type, both mutants showed no or marginal activity for 4-NQO, suggesting its essential role in the reduction activity of the nitrocompound substrate [Fig. 1(C)].

Absence of protruding helices

Upon comparison to other nitroreductase structures, Frm2 reveals a distinctive feature near the FMN binding groove that lacks the prominent helical

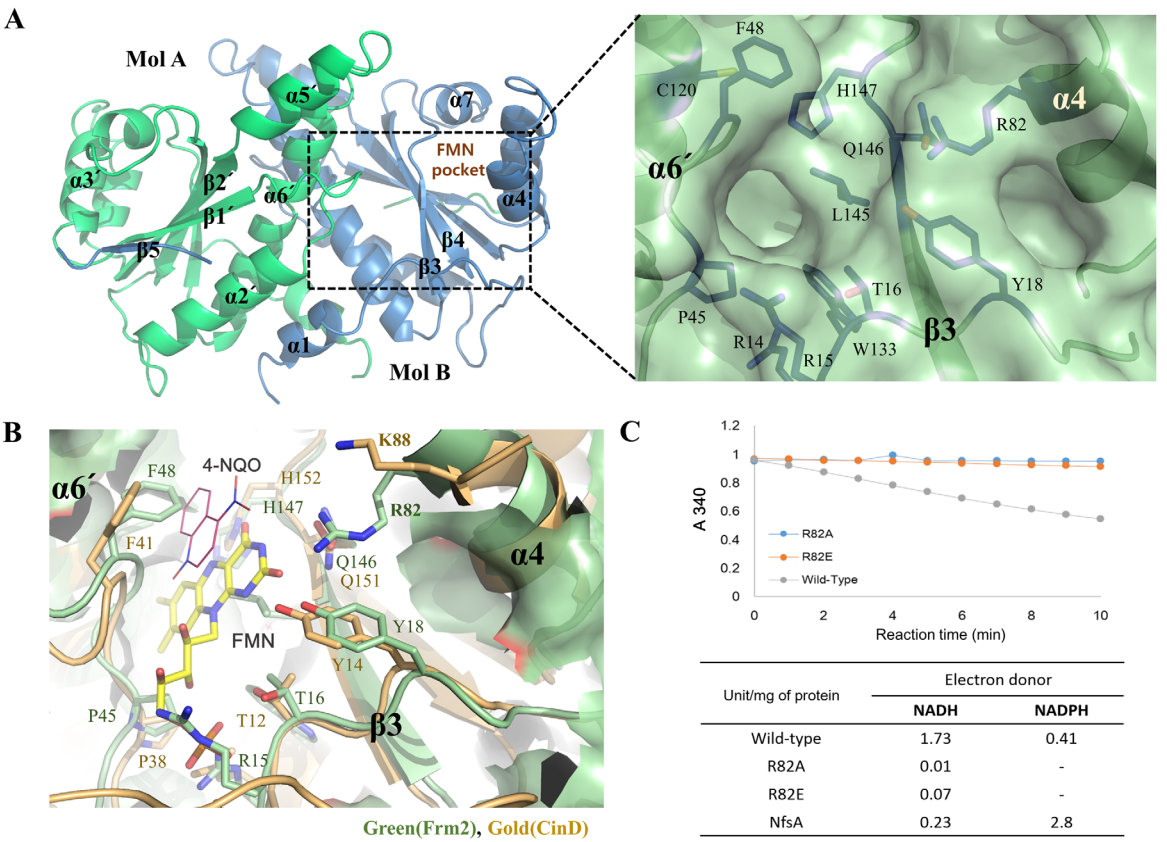

Unit/mg of protein	Electron donor	
	NADH	NADPH
Wild-type	1.73	0.41
R82A	0.01	-
R82E	0.07	-
NfsA	0.23	2.8

Figure 1. Overall structure and active site of Frm2. (A) Homodimeric arrangement of Frm2 (Mol A: green, Mol B; blue) with labeled secondary structures. The α-helix 8 located at the C-terminal end is not visible in the structure. FMN binding pocket is located in dotted box. The key residues in the FMN binding groove and active site are shown as sticks in the enlarged surface diagram. (B) Comparison of the active site. Models of 4-NQO and FMN are superposed to the active site pocket of Frm2 (green) based on the substrate bound CinD complex structure (pdb 4bnb, gold). The positively conserved residue Arg82, corresponding to Lys88 in CinD, is positioned in close proximity to NO_2 moiety of 4-NQO. (C) Nitroreductase activities are shown by the reduction of NADH with the 4-NQO substrate for wild type Frm2 and for mutant proteins of the Arg82 residue (R82A and R82E). Specific activities are indicated in the table. Assays were performed in 1 mL of 50 m*M* Tris–Hcl (pH 7.5) containing 10 μM FMN, 0.2 m*M* NAD(P)H and 0.05 m*M* nitrocompounds. Reactions were started by adding 100 nM of enzyme, and changes in absorbance were measured for 20 min at room temperature. One unit is defined as μmoles NAD(P)H per min.

domains observed in Groups A or B proteins. The Dali server indicated that Frm2 has structural homologues to bacterial nitroreductases such as the CinD from *Lactococcus lactis* and an uncharacterized protein from *Bacillus cereus* with 1.5 Å r.m.s.d. (21.6 *Z* score, over 189 Cα atoms) and 1.7 Å r.m.s.d. (21.4 *Z* score, over 199 Cα atoms), respectively.[14] It also exhibits overall similarity to the minimal nitroreductase YdjA from *E. coli* with 3.5 Å r.m.s.d over 133 aa.[15] We found five structures in the PDB database (2wqf, 1ywq, 2ifa, 2i7h, 3bm1) that share the common minimal architecture without the protruding helical motifs in the FMN binding entrance. Among those structures, enzymatic characterization was reported only for CinD.[13] Previously, these protruding helical motifs were suggested to confer substrate specificity with a role in binding NAD(P)H molecules.[16] In Frp of Group A, for example, three helices of I, J, and K located in the extra C-terminus occupy the front space of the binding groove where residues in these helices such as Arg225, Arg133, and Asn134 interact with the nicotinamide moiety, and the positively charged side chains of Lys167 and Arg15 interact with the pyrophosphate of NADPH[17] [Fig. 2(A)]. For NfnB of Group B, two α-helices of C and D, inserted between the α4- and α5-helix in Frm2, constitute a small domain in the equivalent position near the FMN pocket entrance. The purine ring of the adenosine moiety stacks between the side chains of Tyr113 and Arg120 of the helix, while the 2′-phosphate group of NADPH points externally with only a salt bridge to Arg105, resulting in the inefficient discrimination between NADPH and NADH[18] [Fig. 2(B)]. Because the nicotinamide ring of NAD(P)H and the isoalloxazine ring of the FMN cofactor should be positioned close enough for interaction, the absence of the secondary helical elements that bind to the NAD(P)H molecule suggests a significantly altered binding mode in the interaction with the reducing agent in Frm2 [Fig. 2(C)]. Based

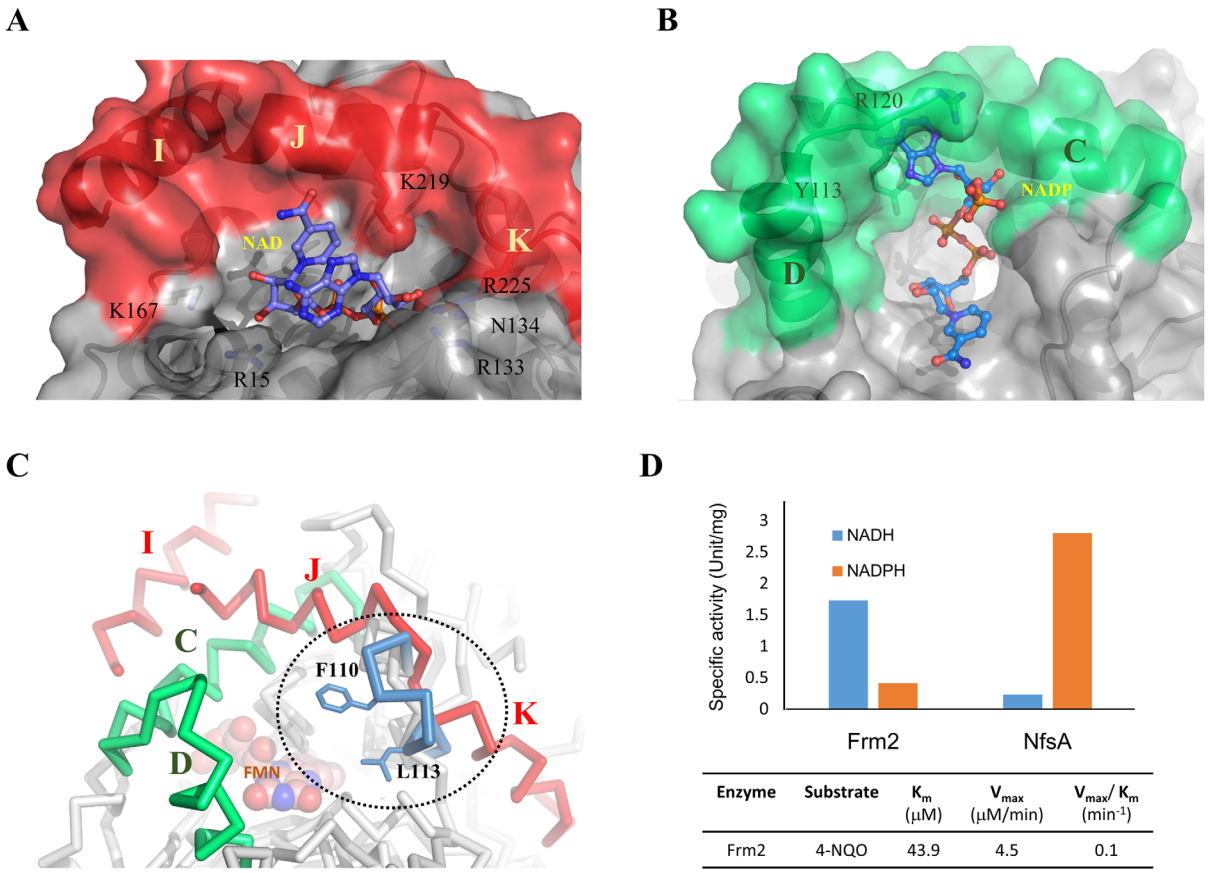

Enzyme	Substrate	K_m (μM)	V_{max} (μM/min)	V_{max}/K_m (min^{-1})
Frm2	4-NQO	43.9	4.5	0.1

Figure 2. Protruding helical elements in the NAD(P)H interaction. (A) Frp structure from *Vibrio harveyi* in Group A has helices of I, J, and K (red) in the C-terminus for interaction to NADPH (pdb 2bkj). The unusually folded structure of nicotinamide adenine dinucleotide is located in proximity to the protruding helices. (B) NfnB structure from *Mycobacterium smegmatis* in Group B has helices of C and D (green) for the nondiscriminative interaction to NADPH (pdb 2wzw). (C) The minimal architecture of Frm2 without the protruding helices suggests an alternative binding mode for the reducing agent. (D) Frm2 utilizes mainly NADH, whereas NfsA in Group A utilizes the NADPH molecule. Kinetic parameters associated to substrate consumption in wild type are shown in a table.

on the proximal geometry, Phe110 and Leu113 in the loop between α4- and α5-helix may be involved in the binding in Frm2. Intriguingly, Frm2 primarily utilizes NADH as an electron donor and shows only marginal activity with NADPH[12] [Fig. 2(D)]. CinD exhibits four times higher activity with NADH compared to NADPH.[13] Recently, a fungal nitroreductase from *Taiwanofungus camphorate*, having a 35% sequence identity to Frm2, was characterized to show significantly high activity with NADH.[19] This finding suggests that nitroreductases in this architecture may take a binding mode that favor NADH molecule. It would be interesting to determine whether other homologues, previously known to be nitroreductase-like A proteins,[10,11] also preferably utilize NADH over NADPH.

In summary, the Frm2 structure reveals that it has minimal architecture with a simple and wide open configuration in the FMN binding entrance. The conserved Arg82 is essential for enzymatic activity in the reduction of 4-NQO. The absence of the secondary elements involved in the binding to NAD(P)H in Groups A or B in the Type I nitroreductase family suggest that Frm2 may take an altered binding mode for the reducing compound interaction. Frm2 and some bacterial nitroreductase-like A proteins with the minimal architecture could be classified into a new group, possibly related to the primary use of NADH.

Materials and Methods

Cloning and protein expression and purification

The gene encoding Frm2 (Alias; YCLX08C) was amplified by PCR from *S. cerevisiae* genomic DNA. The easy cloning kit (enzynomics) was used for complete construction of the pET28a vector. The constructed vector was transformed into *E. coli* BL21-DE3, which was cultured at 17°C in Luria–Bertani (LB) broth media with kanamycin (30 mg/mL) for 16 h. The cells were collected by centrifugation (8000*g*, 30 min), resuspended in lysis buffer (50 m*M* HEPES at pH 7.9, 500 m*M* NaCl, 1 m*M* EDTA, 1% NP40, and 10% glycerol, 1 m*M* DTT), and sonicated

Table I. *Data Collection and Structure Refinement Statistics*

Data collection	Native Frm2
X-ray source	7A, PAL
Space group	*P32*
Unit cell dimensions	
a, b, c (Å)	60.04, 60.04, 110.67
α, β, γ (°)	90, 90, 120
Wavelength (Å)	0.97918
Resolution (Å)	50–3.0
R_{sym} (%)[a,b]	13.3 (43.1)[b]
$I/\sigma(I)$	7.4 (1.7)
Completeness (%)	97.2 (91.8)
Redundancy	5.6 (3.2)
Solvent content (%)	53.6
No. of copies in ASU	2
Refinement	
Resolution (Å)	26.3–3.0
No. of reflections	8754
R_{work}/R_{free} (%)[c]	21.9/26.8
R.m.s deviations	
Bond lengths (Å)/angles (°)	0.006/1.2
Average B factor	44.3
No. of nonhydrogen atoms	2760
No. of water molecules	9
Ramachandran plot (%)	
Favored region	82.7
Allowed region	16.7

[a] Numbers in parentheses are statistics from the highest resolution shell.
[b] $R_{sym} = |I_{obs} - I_{avg}|/I_{obs}$, where I_{obs} is the observed individual reflection.
[c] $R_{work} = |F_0| - |F_c|\,|/|F_0|$, where F_0 and F_c are the observed and calculated structure factor amplitudes, respectively. R_{free} was calculated using 5% of the data.

(Vibra-cell VCX600; Sonics and Materials, USA) in an ice bath for 4 min. The supernatant was clarified by centrifugation (10000*g*, 30 min, 4°C) and purified using a nickel-affinity chromatography (Peptron).

Crystallization and data collection

Frm2 crystallization trials were conducted using the sitting drop method at 18°C. We mixed 20 mg/mL of Frm2 solution with an equal volume of crystallization reservoir solution containing 20% (w/v) polyethylene glycol (PEG) 4000 and 0.2*M* ammonium citrate tribasic pH 7.0, 0.1*M* Tris pH 8.5. Before the data were collected, the crystals were cryo-cooled to 95 K using a cryoprotectant consisting of a mother liquor supplemented with 25% glycerol. The diffraction data set was collected using the MX6C synchrotron beamlines at the Pohang Accelerator Laboratory (Pohang, Korea). The crystals diffracted to a resolution of 2.9 Å, and the data were collected with rotations of crystal spanning 365° at 1° intervals.

Structure determination and refinement

Diffraction data were processed and scaled using HKL2000. The structure was determined by the molecular replacement method using the Phaser CCP4[20] suite and the structure of the CinD of *L.lactis* (PDB code 2wqf) as a searching model. The resultant model was refined in conjunction with model rebuilding using CNS.[21] COOT was used for stereographic manual refinement and model building.[22] The structure was validated with PROCHECK.[23] Sequence alignments and structure-based sequence alignments were performed using Clustal W.[24] Molecular images, including cartoon and stick representations, were produced using PyMOL (http://www.pymol.org/). The crystallographic data statistics are summarized in Table I.

Nitroreductase activity assay of Frm2

Steady-state enzyme kinetics with purified NTRs were assessed spectrophotometrically at 340 nm (based on the equal absorption of $NAD(P)^+$ reduction products of NAD(P)H at this wavelength). Assays were performed in 1 mL of 50 m*M* Tris–Hcl (pH 7.5) containing 10 μM FMN, 0.2 m*M* NAD(P)H and 0.05 m*M* nitrocompounds. Reactions were started by adding 100 nM of enzyme, and changes in absorbance were measured for 20 min at room temperature. Michaelis–Menten curve fitting were performed using Sigmaplot 10.0 (Systat Software, Richmond, CA). The NfsA, encoding the major oxygen-insensitive nitroreductase in *E. coli*, was used as a positive control.

Accession numbers

The atomic coordinates and structure factors (4urp) have been deposited in the Protein Data Bank, Research Collaboratory for Structural Bioinformatics, Rutgers University, New Brunswick, NJ (http://www.rcsb.org).

Acknowledgments

This research was supported in part by the National Research Foundation of Korea (NRF) funded by the Ministry of Science, ICT and Future Planning (2010-0011602/2012K1A3A1A30055018).

References

1. Watanabe M, Nishino T, Takio K, Sofuni T, Nohmi T (1998) Purification and characterization of wild-type and mutant "classical" nitroreductases of *Salmonella typhimurium*. L33R mutation greatly diminishes binding of FMN to the nitroreductase of *S. typhimurium*. J Biol Chem 273:23922–23928.
2. Race PR, Lovering AL, Green RM, Ossor A, White SA, Searle PF, Wrighton CJ, Hyde EI (2005) Structural and mechanistic studies of *Escherichia coli* nitroreductase with the antibiotic nitrofurazone. Reversed binding orientations in different redox states of the enzyme. J Biol Chem 280:13256–13264.
3. Padda RS, Wang C, Hughes JB, Kutty R, Bennett GN (2003) Mutagenicity of nitroaromatic degradation compounds. Environ Toxicol Chem 22:2293–2297.
4. Spain JC (1995) Biodegradation of nitroaromatic compounds. Ann Rev Microbiol 49:523–555.

5. Traversi D, Degan R, De Marco R, Gilli G, Pignata C, Villani S, Bono R (2009) Mutagenic properties of PM2.5 urban pollution in the northern Italy: the nitrocompounds contribution. Environ Int 35:905–910.
6. Bryant C, DeLuca M (1991) Purification and characterization of an oxygen-insensitive NAD(P)H nitroreductase from *Enterobacter cloacae*. J Biol Chem 266:4119–4125.
7. Bryant DW, McCalla DR, Leeksma M, Laneuville P (1981) Type I nitroreductases of *Escherichia coli*. Can J Microbiol 27:81–86.
8. Peterson FJ, Mason RP, Hovsepian J, Holtzman JL (1979) Oxygen-sensitive and -insensitive nitroreduction by *Escherichia coli* and rat hepatic microsomes. J Biol Chem 254:4009–4014.
9. Race PR, Lovering AL, White SA, Grove JI, Searle PF, Wrighton CW, Hyde EI (2007) Kinetic and structural characterisation of *Escherichia coli* nitroreductase mutants showing improved efficacy for the prodrug substrate CB1954. J Mol Biol 368:481–492.
10. de Oliveira IM, Henriques JA, Bonatto D (2007) *In silico* identification of a new group of specific bacterial and fungal nitroreductases-like proteins. Biochem Biophys Res Commun 355:919–925.
11. de Oliveira IM, Zanotto-Filho A, Moreira JC, Bonatto D, Henriques JA (2010) The role of two putative nitroreductases, Frm2p and Hbn1p, in the oxidative stress response in Saccharomyces cerevisiae. Yeast 27: 89–102.
12. Bang SY, Kim JH, Lee PY, Bae KH, Lee JS, Kim PS, Lee do H, Myung PK, Park BC, Park SG (2012) Confirmation of Frm2 as a novel nitroreductase in *Saccharomyces cerevisiae*. Biochem Biophys Res Commun 423: 638–641.
13. Mermod M, Mourlane F, Waltersperger S, Oberholzer AE, Baumann U, Solioz M (2010) Structure and function of CinD (YtjD) of *Lactococcus lactis*, a copper-induced nitroreductase involved in defense against oxidative stress. J Bacteriol 192:4172–4180.
14. Holm L (2010) Rosenstrom P. Dali server: conservation mapping in 3D. Nucleic Acids Res 38:W545–W549.
15. Choi JW, Lee J, Nishi K, Kim YS, Jung CH, Kim JS (2008) Crystal structure of a minimal nitroreductase, ydjA, from *Escherichia coli* K12 with and without FMN cofactor. J Mol Biol 377:258–267.
16. Kobori T, Sasaki H, Lee WC, Zenno S, Saigo K, Murphy ME, Tanokura M (2001) Structure and site-directed mutagenesis of a flavoprotein from *Escherichia coli* that reduces nitrocompounds: alteration of pyridine nucleotide binding by a single amino acid substitution. J Biol Chem 276:2816–2823.
17. Chung HW, Tu SC (2012) Structure–function relationship of *Vibrio harveyi* NADPH-flavin oxidoreductase FRP: essential residues Lys167 and Arg15 for NADPH binding. Biochemistry 51:4880–4887.
18. Manina G, Bellinzoni M, Pasca MR, Neres J, Milano A, Ribeiro AL, Buroni S, Skovierová H, Dianišková P, Mikušová K, Marák J, Makarov V, Giganti D, Haouz A, Lucarelli AP, Degiacomi G, Piazza A, Chiarelli LR, De Rossi E, Salina E, Cole ST, Alzari PM, Riccardi G (2010) Biological and structural characterization of the Mycobacterium smegmatis nitroreductase NfnB, and its role in benzothiazinone resistance. Mol Microbiol 77:1172–1185.
19. Chen CC, Ken CF, Wen L, Chang CF, Lin CT (2012) Taiwanofungus camphorata nitroreductase: cDNA cloning and biochemical characterisation. Food Chem 135: 2708–2713.
20. McCoy AJ, Grosse-Kunstleve RW, Adams PD, Winn MD, Storoni LC, Read RJ (2007) Phaser crystallographic software. J Appl Crystallogr 40:658–674.
21. Brünger AT, Adams PD, Clore GM, DeLano WL, Gros P, Grosse-Kunstleve RW, Jiang JS, Kuszewski J, Nilges M, Pannu NS, Read RJ, Rice LM, Simonson T, Warren GL (1998) Crystallography and NMR system: a new software suite for macromolecular structure determination. Acta Crystallogr D 54:905–921.
22. Emsley P, Cowtan K (2004) Coot: model-building tools for molecular graphics. Acta Crystallogr D 60:2126–2132.
23. Morris AL, MacArthur MW, Hutchinson EG, Thornton JM (1992) Stereochemical quality of protein structure coordinates. Proteins 12:345–364.
24. Thompson JD, Gibson TJ, Higgins DG (2002) Multiple sequence alignment using ClustalW and ClustalX. Current protocols in bioinformatics/editoral board, Andreas D. Baxevanis [et al.] Chapter 2:Unit 23.